Neptunium(V) transport in granitic rock: A laboratory scale study on the influence of bentonite colloids

Elo, O.; Hölttä, P.; Kekäläinen, P.; Voutilainen, M.; Huittinen, N.;

Originally published:

January 2019

Applied Geochemistry 10331(2019), 31-39

DOI: https://doi.org/10.1016/j.apgeochem.2019.01.015

Perma-Link to Publication Repository of HZDR:

https://www.hzdr.de/publications/Publ-27285

Neptunium(V) transport in granitic rock: A laboratory scale study on the influence of bentonite colloids

O. Elo[1*], P. Hölttä[1], P. Kekäläinen[1], M. Voutilainen[1], N. Huittinen[2]

[1] Department of Chemistry, Radiochemistry, University of Helsinki, P.O. Box 55, FIN-00014 University of Helsinki, Finland

[2]Helmholz-Zentrum Dresden-Rossendorf, Institute of Resource Ecology, Bautzner Landstr. 400, 01328, Dresden, Germany

*corresponding author

e-mail: outi.elo@helsinki.fi

Abstract

In the present study neptunium(V) uptake by crystalline granitic rock (Kuru Grey granite) and the role of stable and mobile bentonite colloids (MX-80) on the migration of neptunium(V) was investigated. Two different experimental setups were utilized, batch-type experiments under stagnant conditions and column experiments under flowing water conditions. The uptake of 10^{-6} M neptunium(V) by 40 g/L crushed granite in 10 mM $NaClO_4$ was found to be pH-dependent, whereas neptunium(V) uptake by MX-80 bentonite colloids (0.08-0.8 g/L) was pH-independent up to a pH-value of approximately 11. Column experiments were conducted in the presence and absence of colloids at two pH values (pH = 8 and 10) and two flow rates (0.3 and 0.8 mL/h) in 10 mM $NaClO_4$. The injected neptunium(V) concentration was 2×10^{-4} M and the colloid concentration ranged from 0.08 – 0.32 g/L. The properties of the flow field in the columns were investigated with a conservative chloride tracer, at the same two flow rates of 0.8 and 0.3 mL/h. The resulting breakthrough curves were modeled using the analytical solution of advection–matrix diffusion equation. A tailing of neptunium(V) breakthrough curves in comparison to the conservative tracer was observed, which could be explained by a slightly higher retardation of neptunium(V) in the column caused by sorption on the granite. The sorption was in general lower at pH 8 than at pH 10. In addition, the tailing was almost identical in the absence and presence of MX-80 bentonite colloids, implying that the influence of colloids on the neptunium(V) mobility is almost negligible.

Keywords: *Neptunium(V); Bentonite colloids, Granitic rock, Sorption; Column experiments*

Highlights

- The influence of MX-80 bentonite colloids on neptunium(V) migration in granitic media was investigated.
- Sorption of neptunium(V) on granite was found to be pH-dependent, while MX-80 colloids showed a pH-independent uptake of neptunium(V).
- Neptunium(V) migration in the absence and presence of MX-80 bentonite colloids was investigated in solid granite drill core columns.
- Drill core column experiments were modeled using the analytical solution of advection–matrix diffusion equation in cylindrical coordinates.
- A clear influence of bentonite colloids on neptunium(V) breakthrough was not observed.

1 INTRODUCTION

Several studies have shown that colloid-facilitated transport of radionuclides could have a significant impact on radionuclide migration from hazardous waste sites (Buddemeier and Hunt, 1988; Hursthouse et al., 1991; Kersting et al., 1999; Novikov et al., 2006) and from natural uranium deposits (Short et al., 1988; Vilks et al., 1993). The influence of smectite colloids on the migration of radionuclides in a granitic fracture zone in has been investigated within the Colloid and Radionuclide Retardation experiment (CRR) and the Colloid Formation and Migration (CFM) project (Geckeis et al., 2004; Schäfer et al, 2012; Huber et al., 2011). Laboratory-scale experiments have further shown that the transport of various cationic and anionic metals in porous and fractured media are influenced by the presence of colloids (Ryan and Elimelech, 1996; Artinger et al., 1998; Puls and Powell 1992; Torok et al., 1990; Buckau et al., 2000; Vilks and Baik, 2001; Alonso et al., 2006) depending on the colloid particle size, ground water composition, flow rate, ionic strength, and quantity.

Colloids in natural waters are generated by erosion, geochemical alteration of minerals and through precipitation (Degueldre, 1996). In addition, colloids could form from various natural and engineered barriers in future nuclear waste repositories through erosion of the bentonite clay buffer, copper or steel containers, grouting materials, and the uranium fuel itself (Laaksoharju and Wold, 2005; Finn et al., 1994; Missana et al., 2003; Baik et al., 2007). In this context, several studies have been conducted, both in the absence and presence of colloids, to understand the migration of various radioactive contaminants under future repository conditions and to gain an insight into the potential role of colloids as mobile solid phases for enhanced radionuclide transport in the geosphere.

In the following discussion we will focus on the role of bentonite colloids on radionuclide migration. Bentonite is an important part of engineered barrier systems (EBS) and will be used either as single phase or mixed phase (typically mixed with rock or sand) buffer and backfill

material in different repository concepts for spent nuclear fuel (SNF) (Hummel, 2008). Bentonite has been chosen as an EBS component due to favorable properties such as a low hydraulic conductivity, its swelling ability, and high specific surface area allowing for efficient uptake of potential released radionuclides from the SNF (Missana et al., 2003; 2011). Drawbacks of the buffer material are related to its sensitivity towards the overall salt content of the ground water, where colloid generation has been shown to occur for ionic strengths below the critical coagulation concentration (CCC) (García-García et al., 2007; Tombácz and Szekeres, 2004; Lagaly and Ziesmer, 2003). Such ionic strengths and the subsequent formation of stable and mobile bentonite colloids from the EBS could be reached when the meltwater dilutes the ground water after a possible glacial period. A combination of mobile bentonite colloids and their strong sorption capacity may lead to an unwanted, enhanced mobility of released radionuclides in the geosphere. In general, strong retention on the clay material has been demonstrated for radionuclides in the tri- and tetravalent oxidation states (Zhao et al. (2008), Huber et al. (2011), Verma et al. (2014), Begg et al. (2015)), while sorption of hexavalent radionuclides, such as uranium(VI), occurs readily but seems to depend on both the bentonite material as well as the solution conditions (Missana et al. (2004), Bachmaf et al. (2008), Ren et al. (2010), Huber et al. (2011), Zong et al. (2015)). Uptake studies conducted with pentavalent actinides such as neptunium(V) or plutonium(V) are rather scarce, however, sorption isotherm data show that moderate uptake of neptunium(V)/plutonium(V) occurs in the alkaline pH range (Sabodina et al. (2006), Begg et al. (2015), Li et al. (2015)) and that sorption can be enhanced in the presence of Fe-impurities in the bentonite solid (Verma et al. (2017)). In addition to the batch-type experiments, an enhanced radionuclide mobility due to the presence of bentonite colloids under flowing ground water conditions has been observed to take place for tri- and tetravalent radionuclides and their inactive analogues (Möri et al. (2003), Schäfer et al. (2004), Geckeis et al. (2004), Missana et al. (2008), Dittrich et al. (2015)). The situation is very different for both neptunium(V) and uranium(VI), where close to no impact of bentonite

colloids on the breakthrough properties of these radioelements has been found (Möri et al. (2003), Schäfer et al. (2004), Geckeis et al. (2004)). For both radionuclides an inconclusive breakthrough behavior, requiring more interpretation, was found in Möri et al. (2003), while the breakthrough of both elements investigated in Geckeis et al. (2004) was faster than observed for the conservative tracer (I^-). It was assumed that the rapid flow through open channels did not allow for sufficient interaction between the tracers and rock surface. Further attempts to explain neptunium(V) migration through fractured rock in the presence of colloids have, to our knowledge, not been made, implying that definite conclusions about the fate of neptunium in the presence of colloids cannot be drawn. As Np-237, due to its long half-life (2.144×10^6 a), is considered as a significant dose contributor in the SNF repository after 100 000 years (Hursthouse et al., 1991; Kaszuba and Runde, 1999; Zhao et al., 2014), understanding the migration behavior of neptunium(V) and the potential influence of colloid transport in the geosphere is mandatory.

Thus, the present study aims at describing neptunium(V) uptake by crystalline granitic rock and bentonite colloids under stagnant conditions in batch-type experiments and the role of stable and mobile bentonite colloids on the migration of neptunium(V) through intact granite rock columns under flowing water conditions. The materials used in this study are bentonite colloids prepared from MX-80 bentonite and Kuru Grey granitic rock. Neptunium(V) sorption on these solid phases under stagnant conditions was studied as a function of pH, solid concentration, and neptunium(V) concentration. The column experiments were conducted under ambient air both in the absence and presence of bentonite colloids. The drill core column experiments were modeled using an analytical solution of advection–matrix diffusion equation. The modeling aims as describing the flow field in the experiments in order to better understand the behavior and interaction of neptunium(V) with the rock matrix and the bentonite colloids.

2 MATERIALS AND METHODS

2.1 MX-80 colloids

The MX-80 bentonite used in this study is sodium-rich Wyoming Volclay-type bentonite provided by B^+Tech. The bentonite has been thoroughly characterized by Kumpulainen and Kiviranta (2010) and it was used as a source of bentonite colloids in the present study. The clay consists of 79.1 % smectite, 7.5 % muscovite, 4.4 % quartz, 3.1 % calcite, 1.7 % plagioclase and minor amounts of other accessory minerals (Kumpulainen and Kiviranta, 2010). The cation exchange capacity (CEC) is 0.89 eq/kg (Kumpulainen and Kiviranta, 2010) and the BET surface area was measured to be 28.9 m^2/g (this study). The chemical composition and CEC were analyzed from the solid Volclay bentonite powder, hence, slight differences in both the chemical composition and the CEC of the colloid suspension used in this study may exist. The elemental composition of the MX-80 bentonite colloidal fraction (25-450 nm) has been analyzed earlier by Lahtinen et al. (2010) using ICP–MS. The calcium concentration was below limit of quantitation suggesting a homoionic form (Na^+) of the colloid suspension.

The MX-80 colloid solutions were prepared by mixing 5 g of solid MX-80 bentonite powder and 500 mL of 10 mM $NaClO_4$. In batch sorption experiments where a constant pH was required, the 10 mM $NaClO_4$ background electrolyte was buffered either to pH 8 with 10 mM TRIS (tris-hydroxymethyl-aminomethane), or to pH 9 or 10 with 10 mM CHES ((cyclohexylamino)ethanesulfonic acid). Buffered solutions were prepared before addition of MX-80 bentonite to avoid changes in colloid stability caused by changes in ionic strength and pH. Therefore, each colloid suspension was prepared individually leading to dissimilar colloid concentrations in the different batch sorption experiments. In the column experiments, a buffer was not used. The electrolyte solution was in a sealed flask and the pH was checked daily (except during the weekend) and re-adjusted if necessary. The outflow solution in the fraction collector was in

141 contact with ambient air. The pH of the outflow solution was measured before the experiments from
142 the solution collected in a sealed bottle.

143 All bentonite suspensions were allowed to equilibrate under constant shaking for 7 days prior to
144 extraction of the colloidal material. After the equilibration time, the colloidal material was separated
145 by centrifuging the MX-80 solutions for 20 minutes at 12000 x g (12000 rpm). The centrifugation
146 procedure removed particles with a diameter greater than 500 nm, resulting in a mean colloid
147 particle diameter of approximately 200-300 nm, as confirmed by Photon Correlation Spectroscopy
148 (PCS). Both the colloid particle size and the colloid concentration were determined from the
149 centrifuged supernatants. The determination of the colloid concentration is described in the
150 following paragraph.

151 To ensure that the colloids remain stable under the chosen experimental conditions, their stability in
152 10 mM $NaClO_4$ at around pH 8 without a buffer was followed during 53 days. Five parallel samples
153 were sealed in cuvettes for size or Zeta-potential measurements to avoid the effect of CO_2. The
154 colloid particle size distribution and zeta potential were analyzed applying PCS and
155 microelectrophoresis, respectively (Malvern Zetasizer Nano ZS). During the first 30 days, the mean
156 particle diameter was 215 ± 54 nm. Considering the whole follow-up time, the mean particle
157 diameter was 384 ± 87 nm, the mean colloid concentration was 0.13 ± 0.04 g/L and the mean zeta
158 potential value -54.9 ± -6.6 mV, indicating the existence of a stable bentonite colloid dispersion.
159 The colloid concentration, fed through the column and the eluted amount of colloids in the colloid
160 breakthrough fractions was estimated from the PCS measurement parameter "derived count rate"
161 based on the equation given in Fig. 1 (Niemiaho, 2013). In the calibration curve, the colloid
162 concentration was back-calculated from the structural formula of MX-80 based on the aluminum
163 concentration in bentonite colloid dispersions determined with ICP-MS (Agilent 7500ce). The
164 derived count rate is roughly proportional to the concentration of particles and can be used to
165 estimate the relative concentration of colloids even though the correlation between the ICP-MS and

PCS measurements in range < 1g/L is rather uncertain. PCS was also used to follow the overall colloid particle size eluted from the columns.

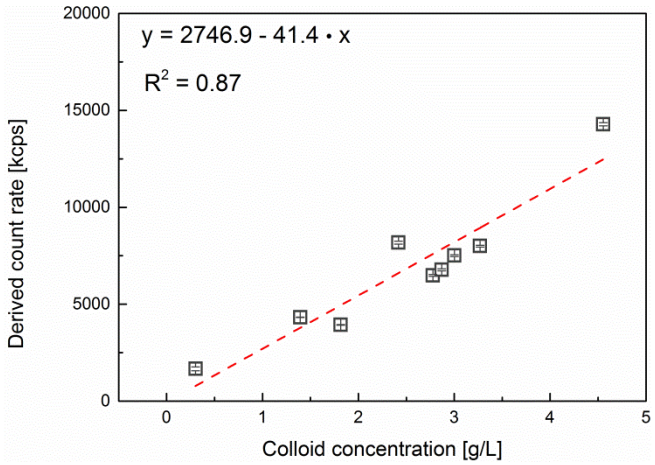

Fig. 1. The correlation between the PCS count rate and the colloid concentration calculated from the aluminum content in bentonite analyzed using ICP-MS (Niemiaho, 2013).

2.2 Kuru Grey granite

Kuru Grey granite was obtained from Kuru Quarry, Tampereen kovakivi Oy, Finland and it has previously been characterized by Hölttä et al. (2004, 2008). The rock matrix of Kuru Grey granite is intact, fine-grained, non-foliated, and equigranular with a density of 2660 kg/m^3. It is composed of 36% potassium feldspar, 35% quartz, 21% plagioclase, and 8% amphibole and micas. The total porosity of the granite is 0.47 % as determined by Jokelainen et al. 2009. For the neptunium(V) batch sorption studies the Kuru Grey granite was crushed and separated into particles that were 0.1 – 1 mm in diameter. For the column experiments an intact drill core Kuru Grey granite column was used.

2.3 Batch sorption experiments

The pH-dependent sorption of neptunium(V) on bentonite colloids was studied both in ambient air and N_2 –atmosphere to investigate the influence of carbon dioxide on the neptunium(V) retention and to simulate anoxic conditions in a final repository. Neptunium(V) sorption on crushed Kuru

Grey granite at constant neptunium(V) concentration of 10^{-6} M and granite concentration of 40 g/L was investigated under ambient air atmosphere only, to simulate the experimental conditions of the column experiments. The neptunium(V) concentration was kept constant at 10^{-6} M, the colloid concentration ranged from 0.08 – 0.8 g/L, depending on the remaining colloid concentration in the supernatant after centrifugation, as explained above (section 2.1). Isotherm studies were performed under constant pH conditions (pH 8, 9, and 10) in N_2-atmosphere as a function of neptunium(V) concentration (10^{-10} to 5×10^{-6} M). TRIS and CHES buffers were used to achieve a constant pH in the experiments. The final colloid concentrations for isotherm experiments at pH 8, 9, and 10 were 0.10, 0.06, and 0.18 g/L, respectively. 10 mM $NaClO_4$ was used as a background electrolyte throughout the experiments. The sample pH was adjusted with 0.01–1 M NaOH and $HClO_4$ solutions. All samples were allowed to equilibrate under constant shaking for 7 days. Thereafter all solid material including the colloids was separated by ultracentrifugation at 690000 g (90000 rpm) allowing the determination of the non-sorbed neptunium(V) concentration from the supernatant. The neptunium(V) concentration was determined by liquid scintillation counting (Quantulus) using α/β – discrimination to separate out the β disintegrations from the Np-237 daughter nuclide Pa-233.

2.4 Column experiments

The effect of bentonite colloids on neptunium(V) migration was studied under flowing water conditions in a drill core column, which has been used earlier in parallel with block-scale experiments to evaluate the simplified radionuclide transport concept (Hölttä et al., 2008).

The intact drill core, 28 cm and 1.4 cm in diameter, was placed in the Glass Econo-Column® 30 cm long and 1.5 cm in diameter, forming a flow channel in the 0.5 mm gap between the rod and tube. The height of the column was adjusted with a Bio-Rad Flow Adaptor. Before the construction of the column, the drill core was cleaned ultrasonically in ethanol to remove dust and any remnants from the drilling procedure. The column experiments were performed under ambient air conditions. The solution was continuously pumped through the column and the effluent was fed to a fraction

collector for determining the break-through of the tracer. The feed solution was replaced with the colloid solution when experiments in the presence of colloids were conducted. Known volumes of tracers were injected in the column through an injection loop with a volume of 12 µL. The total volume of the flow channel in the column is 6.4 mL which is 500 times higher than the volume of injection loop indicating that the tracer pulse is diluted after injection. Flow rates were controlled with a peristaltic pump and determined by collecting and weighing several parallel fractions of the background electrolyte that eluted through the columns in one hour. The experimental setup is presented in Fig. 2.

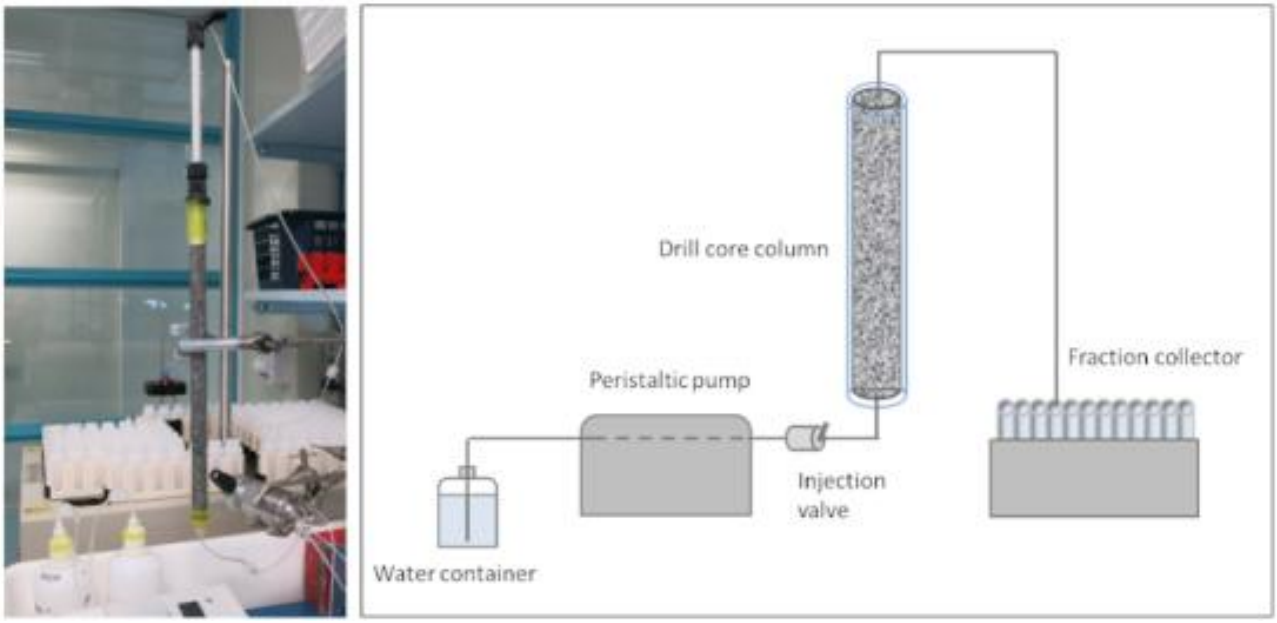

Fig. 2. Experimental set-up and schematic design for the column experiments. The intact 28 cm long drill core with a diameter of 1.4 cm was placed inside a column to form an artificial 0.5 mm aperture flow channel between the core and the column walls.

Matrix diffusion and dispersion are the most important transport mechanisms for radionuclides in a rock matrix (Moreno et al., 1997). Matrix diffusion can only be seen at very slow flow rates (Hölttä et al., 1996, 2008). The flow rates of 0.3 mL/h and 0.8 mL/h for this study were selected based on a previous study with the same drill core column (Hölttä et al., 2008). At the selected flow rates, the transport of the conservative tracer is dominated by hydrodynamic dispersion caused by a

heterogeneous velocity field together with transverse molecular diffusion in the fracture. The transverse diffusion in the fracture smooths out variable flow rates for different streamlines in the circular slit around the core. The effects of matrix diffusion were shown in mobile iodine breakthrough curves only at a very low flow rate of 0.04 mL/h, which excludes the possible disturbing effects of the matrix in this study. The two different flow rates were chosen to elucidate the effect of sorption kinetics on the breakthrough of neptunium(V). The flow field in the column was characterized without colloids using a conservative tracer, chloride (Cl-36). The chloride concentration in the injected tracer volume was 8.7×10^{-2} M, which quickly dilutes inside the column. The total liquid volume in the first 0.5 cm of the column dilutes the injected tracer by a factor of almost 10, which is below the ionic strength of 10 mM $NaClO_4$ used as background electrolyte.

The experimental conditions in terms of pH were selected based on the results obtained in our sorption experiments (see section 3.1). At pH 8, sorption of neptunium(V) on granite is low, and increasing at pH 10. Thus, pH values of 8 and 10 were selected for the column experiments and 10 mM $NaClO_4$ was used as a background electrolyte to ensure comparable conditions to our previous study (Elo et al., 2017) where we investigated neptunium(V) sorption on Na-montmorillonite extracted from the MX-80 bentonite. The rock surfaces in the column were equilibrated by continuously feeding10 mM $NaClO_4$ through the column for several months up to one year. The column was preconditioned at the wanted pH-values by feeding the background electrolyte through the column for at least two weeks prior to experiments. The pH value from the collected solution was determined before the experiment. Neptunium(V) transport through the granite columns was monitored in the absence and presence of bentonite colloids. In both experiments, a rather high neptunium(V) concentration of 2×10^{-4} M was chosen to assure that neptunium could be measured from the collected fractions. However, due to dilution of neptunium(V) inside the column, a concentration of 5×10^{-6} M (maximum concentration used in our isotherm experiments) is reached

already in the first 2 cm (out of 28 cm) in the column. In the experiments conducted in the presence of bentonite colloids, the neptunium(V) tracer was injected into a constant and stable flow of bentonite suspension with a colloid concentration ranging from 0.08 to 0.32 g/L. The eluted neptunium(V)/colloid fraction was collected with a fraction collector and the neptunium(V) concentration was determined from each fraction with LSC as explained above. Prior to the α/β-counting, the colloid concentration in the solution eluted through the column was determined by photon correlation spectroscopy (PCS) and the standard series presented in Fig. 1.

2.5 Analytical modeling

The breakthrough curves of the column experiments with chloride and neptunium(V) in the absence and presence of MX-80 bentonite colloids were modeled using the analytical solution of advection–matrix diffusion equation in cylindrical coordinates (see Kuva et al. 2016 for details). The analytical solution for the problem was constructed using the methods reported previously (Kekäläinen et al., 2011; Kekäläinen. 2014; Kuva et al., 2016). Recently, the model has been further developed so that it is possible to take into account the channeled flow field (Voutilainen et al. 2018). The model takes into account: (i) 1D diffusion in the flow field in direction of advection, (ii) 1D radial diffusion in the rock matrix, (iii) sorption on mineral surfaces in the rock matrix, and (iv) the channeled flow field between the cylindrical sample and the pipe surrounding the sample. The analytical solution was derived for a Dirac delta function input starting from partial differential equations describing the phenomena given above. The equations were solved by first writing them in dimensionless form, finding the eigenvalues which are a combination of Bessel functions in the cylindrical case, and solving the partial differential equations in Laplace space.

As a first step, the effect of the tubes before and after the granite column was subtracted from the total flow-through time. Thereafter the flow velocity was scaled to get the raising part of the

breakthrough curve to the correct position. This was done by keeping the flow rate constant (measured value) and setting part of the water in stagnant state. Here, a scaling factor of 1 means no scaling and values greater than one mean that parts of the channel contains stagnant water (see Fig. 3). Finally, the diffusion coefficient of chloride/neptunium(V) in water was adjusted to enable fitting of the late part of the breakthrough curve. The rock matrix did not affect the breakthrough curves of chloride and, thus, it could be used to characterize the flow field (see Fig. 3). In contrast, the matrix affected the breakthrough curves of neptunium(V) due to moderate sorption on granite. Thus, the K_d of neptunium(V) was adjusted to fit the late part of the breakthrough curves. In Fig. 3 the influence of matrix diffusion (left), K_d (middle), and the stagnant-to- flowing water ratio (right) on the breakthrough curves are demonstrated. The values for porosity and the effective diffusion coefficient of Kuru Grey granite were selected according to previously determined values, i.e. 0.47 % (Jokelainen et al. 2009) and 8×10^{-13} m^2/s (Ikonen et al. 2016), respectively.

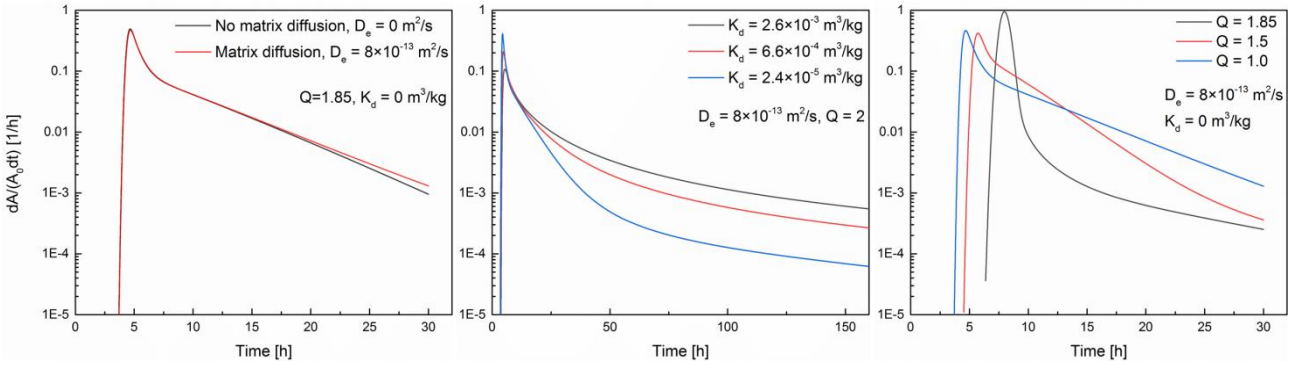

Fig. 3 The influence of the effective diffusion coefficient (left), K_d (middle) and scaling of flow velocity (right) on the breakthrough curves.

3 RESULTS AND DISCUSSION

3.1 Batch sorption experiments

The pH-dependent sorption of neptunium(V) onto MX-80 bentonite colloids and crushed Kuru Grey granite is presented in Fig. 4 as sorption percentages (left) and K_d values (right). Each data point represents the average of duplicate measurements, and the error bars are standard deviations of these measurements.

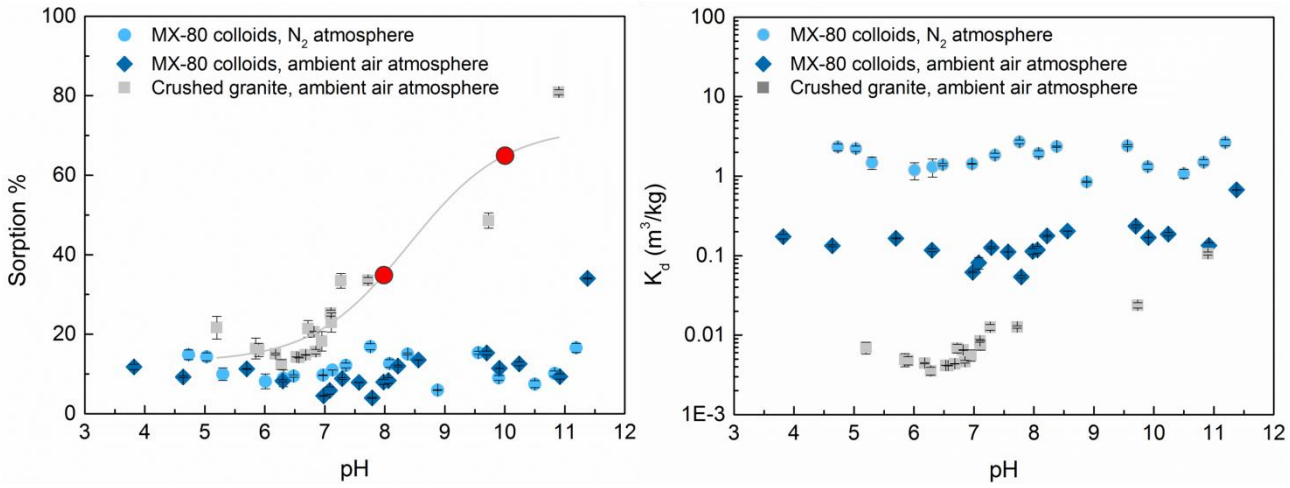

Fig 4. Neptunium(V) sorption on MX-80 colloids in N_2-atmosphere ($c_{colloids}$ = 0.08 g/L), in ambient air atmosphere (0.8 g/L), and on crushed Kuru Grey granite (40 g/L).

The neptunium(V) concentration was 10^{-6} M and background electrolyte 10 mM $NaClO_4$. The data is given both as the sorption percentage vs. pH (left) and K_d vs. pH (right). For crushed granite, a Boltzmann Fit of the sorption percentage vs. pH graph was made to select pH values (red spheres) for the column experiments.

For neptunium(V) uptake by MX-80 bentonite colloids in N_2-atmosphere, the sorption percentage remains almost stable up to a pH-value of 11.2 (16 %, $K_d = 2.6 \pm 0.2$ m^3/kg). In addition, no clear difference in the sorption percentage between N_2-atmosphere and ambient air atmosphere can be seen except at pH 11.4 (34 %, $K_d = 0.671 \pm 0.003$ m^3/kg). This implies that the formation of neptunium(V)-carbonate complexes can be neglected at the chosen experimental conditions (pH ≤

10) in the column experiments which, further, allows us to draw conclusions about the influence of colloids on the neptunium(V) mobility in these experiments. A difference between N_2 and ambient air atmosphere can be seen in the K_d values. This difference is constant over the whole pH-range and cannot, therefore, be attributed to the presence of carbon dioxide which could result in formation of soluble neptunium(V)-carbonate complexes in the neutral to alkaline pH-range. The difference most likely arises from the absolute colloid concentration which is used in the calculation of the K_d-value. As seen in Fig. 1, low colloid concentrations (below 1 g/L) are represented by only one data point in the calibration curve. Therefore, a larger uncertainty is expected for the very low colloid concentration range (such as the 0.08 g/L used in experiments conducted in N_2 atmosphere) in comparison to 0.8 g/L (used at ambient conditions) and beyond. The constant sorption behavior over the entire examined pH-range is not in agreement with our previous studies, investigating neptunium(V) uptake by montmorillonite extracted and purified from MX-80 bentonite by B^+Tech and MX-80 bentonite colloids (Elo 2014, Elo et al. 2017). In those studies, a pH-dependent uptake of neptunium(V) was found, which could be described by the presence of a small amount of ion exchanged neptunium(V) in the acidic to circumneutral pH range and two surface complexes at pH-values above 7. Also, the used solid/liquid –ratio was roughly 3.5 g/L which was the value at the plateau where maximum neptunium(V) sorption was obtained. Furthermore, a K_d value of 2.6 (observed in the present study over the entire investigated pH-range) was obtained for neptunium(V) sorption on montmorillonite only at pH-values exceeding 10. Both the pH-independent behavior and the high K_d obtained in the present study for neptunium(V) sorption on MX-80 bentonite colloids imply, that a large amount of neptunium is adsorbed on the colloids through cation exchange on clay surfaces exhibiting permanent negative charge. This is in line with the overall CEC (0.89 eq/kg), which can hold the overall amount of NpO_2^+ cations present in the clay suspensions, even for the lower colloid concentration of 0.08 g/L. The overall low sorption percentage can be attributed to the low concentration of colloids used in the present study.

However, yet higher colloid concentrations are not expected in natural scenarios and would, thus, not provide a realistic view of their influence on radionuclide mobility in the sub surface environment. In fact, measured colloid concentrations at various underground laboratories such as Äspö, Grimsel, and Gorleben, range from 10^{-6} g/L to some milligrams per liter (Degueldre et al., 1988; Jansson, 2009; Laaksoharju and Wold, 2005; Smith and Degueldre, 1993). In the presence of eroded bentonite, however, colloid concentrations of several hundred milligrams per liter (> 0.1 g/L) have been observed (Jansson, 2009; Missana et al., 2011). Thus, our sorption results for the lower colloid concentration of 0.08 g/L can be expected to lie closest to the range expected in the near-field of a future repository for spent nuclear fuel as a result of bentonite erosion.

Neptunium sorption on the crushed granite increases at pH 7 and above. The maximum sorption percentage remains relatively low (81 %, $K_d = 0.106 \pm 0.005$ m^3/kg at pH 11). Our results differ somewhat from already published studies on neptunium(V) uptake by granite: Kumata and Vandegraaf (1998), Kienzler et al. (2003), and Park et al. (2012) all found neptunium(V) reduction to neptunium(IV) and a subsequent high retention of the reduced species on granite. Despite the presence of amphibole, a mineral that often contains iron in the structure, in the Kuru Grey granite used in the present study, no reduction of neptunium can be deduced from the low overall uptake in the batch sorption studies and the high recovery of neptunium in the column experiments (discussed later in the text).

Due to the pH-independent sorption of neptunium(V) on MX-80 bentonite colloids throughout the investigated pH range, experimental conditions for the column experiments (discussed below in section 3.2) were chosen based on the batch sorption data for crushed granite. Here, moderate sorption of neptunium(V) was obtained in the circumneutral pH range with a slight increase of sorption with increasing pH. Thus, pH values of 8 and 10 were selected for the column studies based on the Boltzmann Fit of the sorption percentage vs. pH graph for crushed granite (see Fig. 4 left).

To investigate the neptunium(V) sorption behavior on MX-80 bentonite colloids at varying neptunium concentrations, which is of relevance in the column experiments where a neptunium(V) concentration gradient can be expected in the injection stage, sorption isotherms at constant pH, as a function of neptunium(V) concentration were conducted. Results are presented in Fig. 5. It can be seen that all three (pH 8, 9, and 10) curves are linear with a slope of 0.9 ± 0.12, implying that close to ideal sorption conditions (characterized by a slope of 1) are maintained over the investigated concentration range.

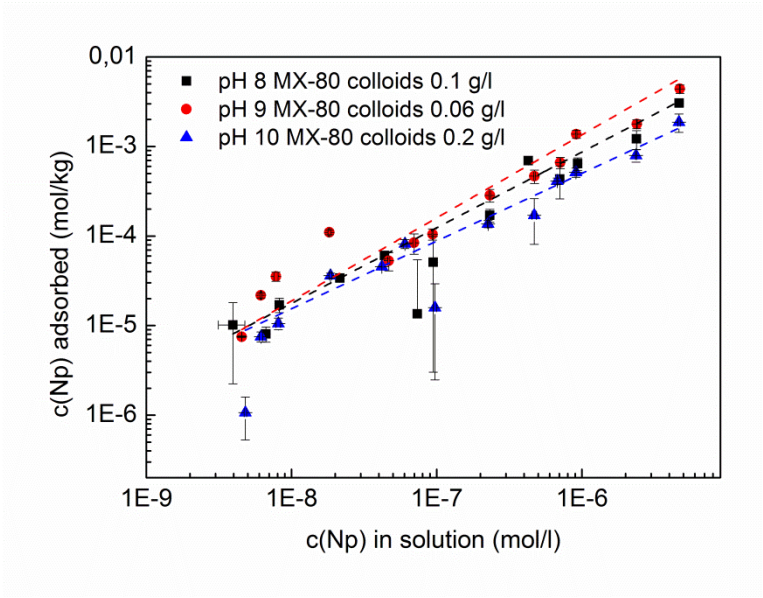

Fig 5. Neptunium(V) sorption isotherms in N_2-atmosphere on MX-80 colloids at pH 8 ($c_{colloids}$ = 0.1 g/L), pH 9 (0.06 g/L) and pH 10 (0.2 g/L). The neptunium(V) concentration is 10^{-9} - 5×10^{-6}.

3.2 Column experiments

3.2.1 Chloride (Cl-36)

The flow through properties of the drill core column were investigated by following the migration of a conservative chloride tracer through the columns at two different flow rates of 0.8 mL/h and 0.25 mL/h (Fig. 6).

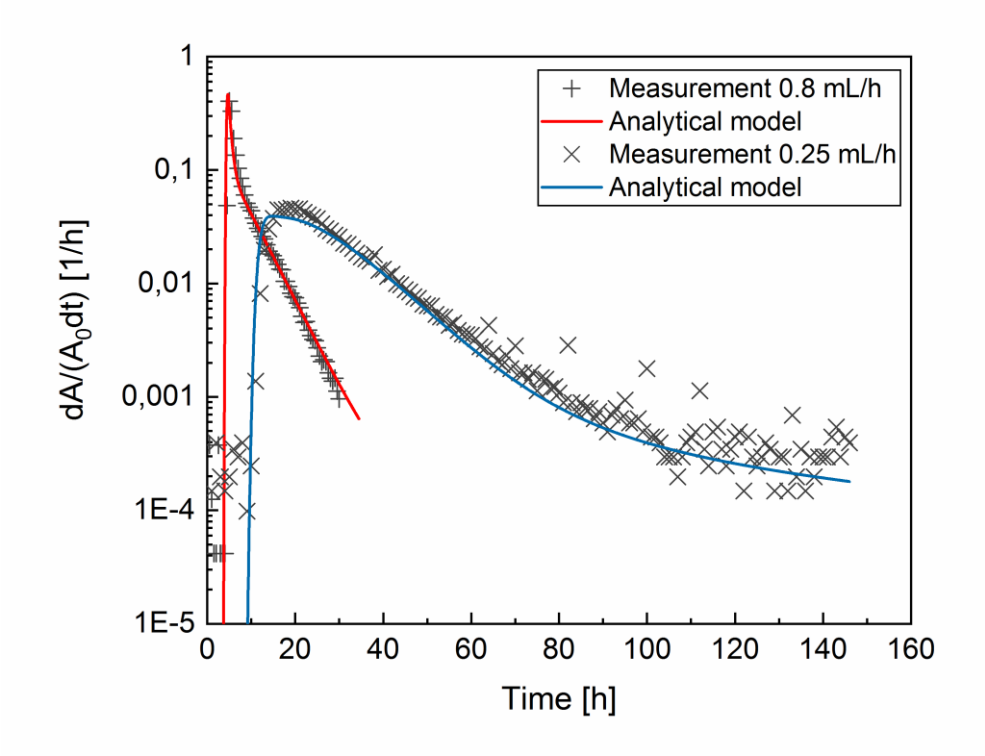

373

374 Fig. 6. Measured and modeled breakthrough curves of chloride in the absence of colloids through
375 the drill core column. The chloride concentration in the injected tracer volume was 8.7×10^{-2} M. The
376 recoveries of the Cl-36 tracer were approximately 100 %.

377

378 In Fig. 6 the breakthrough of chloride can be seen to be governed by the flow velocity. As expected,
379 the breakthrough occurs earlier for the faster flow rate, followed by a slight tailing at both flow
380 speeds, which can be attributed to dispersion in the column as previously shown by Park et al.
381 (2012). The modeled breakthrough curves are in good agreement with the measured ones. The
382 modeling results in terms of velocity scaling and diffusion coefficients for chloride in water are
383 compiled in Table 1.

384 Table 1. The modeling results of measured breakthrough curves of chloride from the drill core
385 column using different flow rates. The results include the velocity scaling and the self-diffusion
386 coefficient of the element in water (D_0).

Element (pH)	Flow rate [mL/h]	Velocity scaling [-]	D_0 [m^2/s]
Cl-36 (8)	0.8	5	3×10^{-9}
Cl-36 (8)	0.25	2.5	3×10^{-9}

387

388 The velocity scaling can be seen to vary from one measurement to another. This may be due to a
389 slight displacement of the sample in the plastic tube resulting in a non-uniform aperture around the
390 sample. The variation in the aperture of flow channels has caused channeling of the flow field. A
391 direct consequence of the non-uniform aperture and the variations in the water flow, are the slightly
392 higher values obtained in the present study for diffusion coefficients for chloride in water in
393 comparison to the published value of 2.0×10^{-9} m^2/s (Bastug and Kuyucak 2005). This compensates
394 the effect arising from a larger interaction between the flowing and stagnant water than with the
395 average aperture. However, the difference between the published and modeled diffusion
396 coefficients for chloride in water is minor when taking into account the robustness of the
397 experiment. In general, such channeling of the flow field is typical in natural systems and in
398 artificial systems for fracture flows.

399 **3.2.2 Neptunium(V) and colloids**

400 Neptunium(V) breakthrough curves for the flow rate of 0.8 mL/h in the absence (red symbols) and
401 presence (blue symbols) of bentonite colloids in the drill core granite column experiments at pH 8
402 and 10 are presented in Fig 7. Results obtained for the flow rate of 0.3 mL/h are presented in Fig. 8.

403

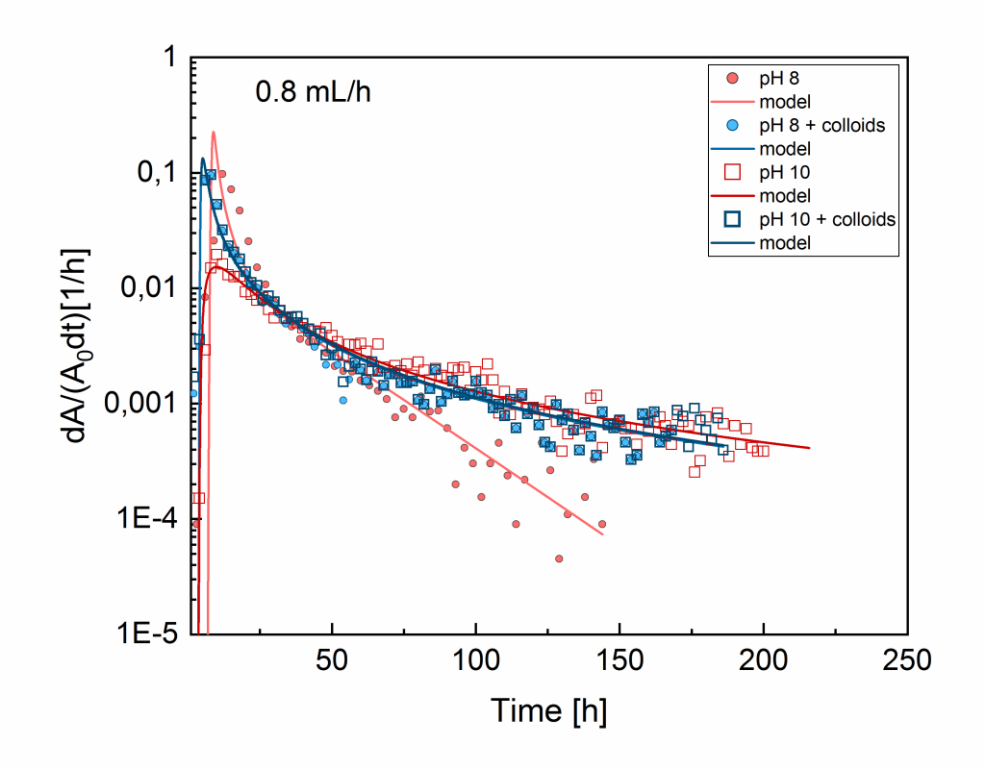

404

405 Fig 7. Measured and modeled breakthrough curves for neptunium(V) through the drill core column
406 at a flow rate of 0.8 mL/h in 10 mM $NaClO_4$, pH 8 (closed symbols) and pH 10 (open symbols) in
407 the absence (red traces) and presence of colloids (blue traces). The neptunium(V) recoveries at pH 8
408 and pH 10 were 95% and 68 %, respectively, in the absence of colloids. In the presence of colloids
409 recoveries of 99% (pH 8) and 98% (pH 10) were obtained.

410

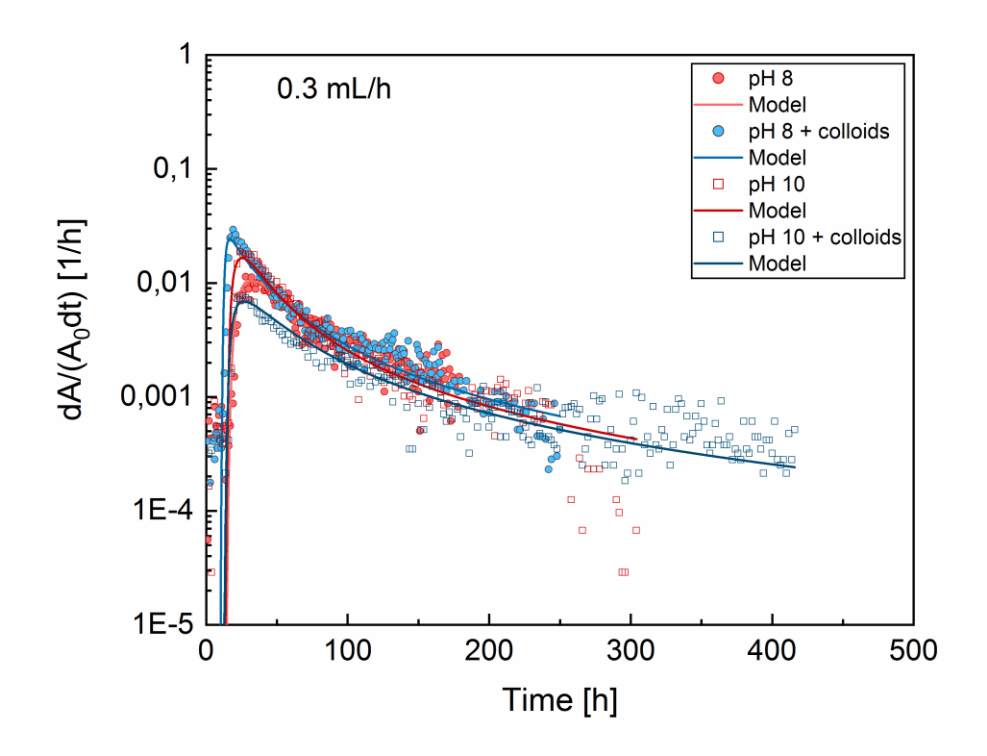

411

412 Fig 8. Measured and modeled breakthrough curves for neptunium(V) through the drill core column,
413 flow rates of 0.3 mL/h in 10 mM $NaClO_4$ pH 8 (closed symbols) and 10 (open symbols) in the
414 absence (red traces) and presence of colloids (blue traces). The neptunium(V) recoveries at pH 8
415 and pH 10 were 96% and 92 %, respectively, in the absence of colloids. In the presence of colloids
416 recoveries of 100% (pH 8) and 60% (pH 10) were obtained.

417 Breakthrough curves for the colloids are presented in Fig. 9. Here, only the results obtained for the
418 flow rate of 0.3 mL/h at pH 8 have been collected together with the neptunium(V) data presented
419 above, by determining the mean particle size and derived count rate with PCS from all collected
420 fractions. The colloid breakthrough curves for the experiments at 0.8 mL/h, pH 8 and 0.3 mL/h, pH
421 10 are results of separate experiments. The colloid concentrations in these experiments were 0.25
422 g/L and 0.32 g/L, respectively. For the flow rate 0.8 mL/h, the recoveries of colloids were 80 ± 9 %
423 during the whole experiment. For the flow rate of 0.3 mL/h, the recoveries fluctuated between 65 %
424 and 98 % in the beginning and thereafter decreased down to 20 % suggesting filtration of colloids
425 into the stagnant areas of the flow channel or tubing. The mean particle sizes stayed constant at 190

± 99 nm (0.8 mL/h) and 220 ± 85 nm (0.3 mL/h) over the whole collection time, which is in line with the results obtained in our colloid stability tests where a constant colloid size of 215 ± 54 nm was maintained over 30 days (720 hours).

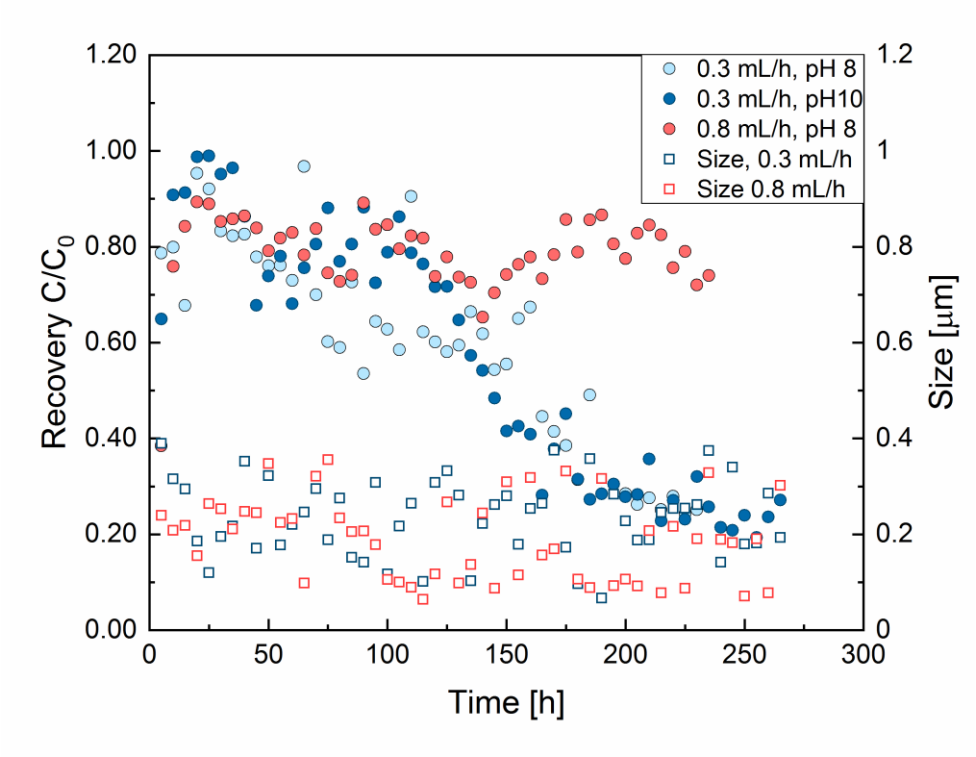

Fig. 9. The breakthrough and mean particle size of colloids. The colloid breakthrough at 0.3 mL/h, pH 8 (light blue spheres, 0.08 g/l) was determined from the neptunium(V) experiment in the presence of colloids. The breakthrough at 0.3 mL/h, pH 10 (0.32 g/l) and 0.8 mL/h, pH 8 (0.25 g/l) (blue and red spheres) as well as mean particle sizes (squares) are determined from separate colloid breakthrough experiments.

3.2.3 Discussion

The modeled neptunium(V) breakthrough curves in the absence and presence of colloids are in good agreement with the measured ones. The modeling results in terms of velocity scaling and diffusion coefficients for neptunium in water are compiled in Table 2.

439 Table 2. The neptunium(V) recoveries and modeling results of measured breakthrough curves from
440 the drill core column using different flow rates. The modeling results include the velocity scaling
441 and the sorption distribution coefficient (K_d). The self-diffusion coefficient of the element in water
442 (D_0) was 3×10^{-9} m^2/s in all cases.

Element (pH)	Flow rate [mL/h]	velocity scaling [-]	K_d [m^3/kg]	Np-237 recovery [%]
Np-237 (8)	0.8	1	8×10^{-5}	95
Np-237 + col (8)	0.8	2	0.003	99
Np-237 (10)	0.8	2	0.004	68
Np-237 + col (10)	0.8	2	0.003	98
Np-237 (8)	0.3	1.5	0.0009	96
Np-237 + col (8)	0.3	2	0.0005	100
Np-237 (10)	0.3	1.5	0.001	92
Np-237 + col (10)	0.3	1.7	0.002	60

443

444 The observed rapid increase of the breakthrough curves obtained for the intact drill core column are
445 mainly governed by the ratio between stagnant and flowing water in the columns. In the
446 experiments conducted at the slower flow rate (Fig. 8), the pre-peak position remains constant in the
447 presence and absence of colloids, while a shift can be seen for the 0.8 mL/h data. The observed
448 differences in this pre-peak position must, thus, originate from slight differences of the drill core
449 position in the plastic tubes during the breakthrough experiments. The modeled breakthrough
450 curves (Figs. 7 and 8) show that the flow field is channeled in the neptunium(V) experiments and
451 that typically about half of the flow channel has flowing water (see Table 2). The raise of the
452 breakthrough curve is not as steep as for chloride. This demonstrates that the flow field cannot be
453 fully modeled with the simple dual flow velocity model as the sorbing nuclide interaction with the

454 rock matrix is stronger than such models predicts. However, in this case the late part of the
455 breakthrough curve cannot be explained by only matrix diffusion into stagnant water and later back
456 to the flowing area and, thus, sorption affects the late part of the breakthrough curve.

457 A higher tail of the breakthrough curves, especially at the flow velocity of 0.8 mL/h, can be seen
458 with increasing pH in the absence of colloids, indicating that neptunium(V) sorbs on the granite
459 surface as also observed in our batch sorption studies on the crushed material (Fig. 4). This can also
460 be seen from the K_d values determined by the modeling (Table 2). Here, the K_d values for
461 neptunium(V) without colloids vary from 8×10^{-5} m^3/kg to 0.004 m^3/kg. These values are between
462 10-200 times lower than obtained in our batch sorption experiments (~0.015-0.030 m^3/kg, pH =8-
463 10). Such a large discrepancy could be a result of a much smaller specific surface area of the
464 column material in comparison to the crushed granite material used in the batch sorption
465 experiments. In Hölttä et al. (1997), a specific surface area of 0.05-0.07 m^2/g and 1.2 m^2/g for intact
466 andcrushed tonalitic rock, respectively, has been reported, i.e. a difference of a factor of
467 approximately 20. Other factors such as a slow sorption kinetic for neptunium(V) uptake by granite,
468 as shown in Park et al. (2012) could play a role in addition to a high reversibility of neptunium(V)
469 sorption under flowing water conditions as was shown for neptunium(V) uptake by montmorillonite
470 in our previous study (Elo et al. 2017). Slow sorption kinetics is supported by the results obtained at
471 pH = 8, where more than 10 times higher sorption distribution coefficient is obtained for the 0.3
472 mL/h flow rate in comparison to the 0.8 mL/h one. This is well in agreement with the overall
473 neptunium(V) column residence time, which was approximately 4 days for 0.3 mL/h and only 25
474 hours for the 0.8 mL/h experiment, whereas the equilibration time for batch sorption studies was 7
475 days. The residence time is taken as the time between tracer injection and elution through the
476 column. At pH = 10 the sorption distribution coefficient is of the same order of magnitude for both
477 flow rates. Whether this is an effect of the stagnant vs. flowing water volume which is
478 systematically higher for the larger flow rate (see tables 1 and 2) or due to changes in the surface

complexation mode (e.g. larger amount of inner-sphere sorption at pH = 10), we cannot deduce based on available data. Thus, for a proper assessment of the underlying reasons between differences in neptunium(V) uptake under stagnant vs. flowing water conditions, detailed understanding of sorption kinetics, reversibility of the sorption reaction, and knowledge of the complexation mechanism on the solid surface are required.

The presence of colloids has almost no influence on the neptunium(V) breakthrough at the slower flow rate of 0.3 mL/h and at the higher pH for the 0.8 mL/h flow rate. Based on our batch sorption data, a constant uptake of neptunium(V) of around 10% of the total neptunium(V) concentration is expected by the bentonite colloids at pH = 8 and 10. In the granite column the sorption percentage is more difficult to assess, as the solid to liquid ratio is unknown. However, a larger amount of neptunium(V) sorption is expected at pH = 10 on the column material, implying that a potential influence of the colloids should be more pronounced at this pH-value. Such an influence, however, is not seen in our column studies. At 0.3 mL/h flow rate, almost no retention of neptunium(V) can be seen on the column material both in the presence and absence of colloids. Therefore, it is difficult to assess if the eluted neptunium(V) in the presence of colloids is associated with the colloids or migrating with the flowing water. The colloid breakthrough behavior at this flow velocity seems to oscillate between 60 and 100 % recoveries before it decreases toward 20%. As already briefly mentioned, this decrease of the colloid breakthrough is most likely a result of filtration of colloids into the stagnant areas of the flow channel or tubing. A similar oscillating breakthrough of neptunium(V) is not observed, which would imply that at least the majority of neptunium(V) is eluted from the column in the aqueous phase. A slight indication for colloid-borne neptunium(V), however, is visible after approximately 160 hours (Fig. 10) when comparing the breakthrough behavior of neptunium(V) with that of the colloids. The abrupt decrease of colloid breakthrough (gray symbols) at this time point is associated with a small kink in the neptunium(V) breakthrough curve (light blue symbols).

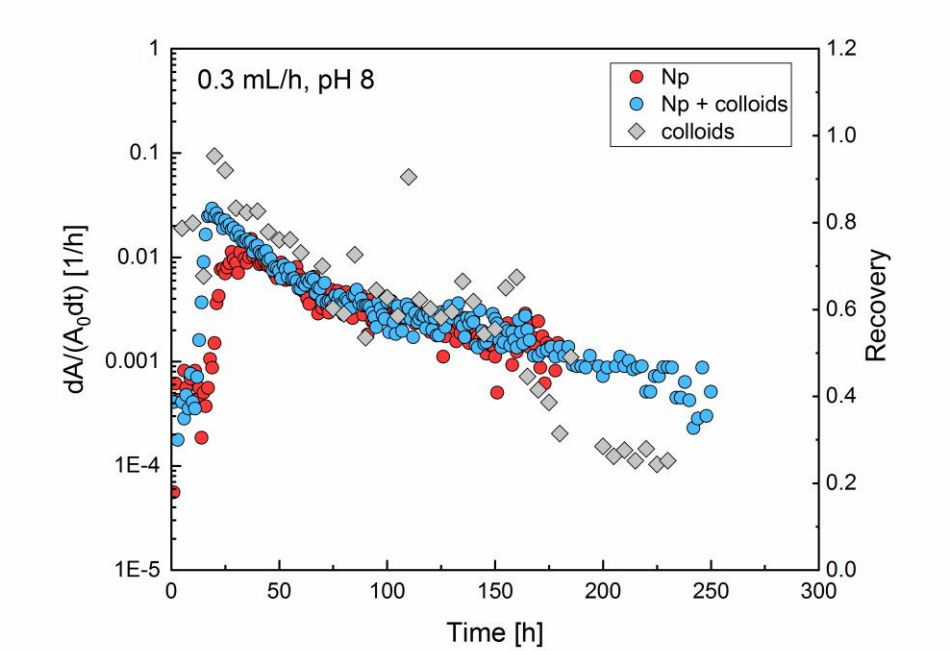

504

505 Fig. 10. Comparison between the breakthrough behavior of neptunium(V) (red and light blue
506 symbols), and the breakthrough (gray symbols) and mean particle sizes (dark blue symbols) of
507 colloids at the flow velocity of 0.3 mL/h and pH = 8.

508

509 At pH 10, both flow rates show a small difference in the sorption distribution coefficient in the
510 presence of colloids. The difference, however, is not systematic, i.e. a slightly lower K_d value is
511 obtained at 0.8 mL/h while the opposite is true at 0.3 mL/h in the presence of bentonite colloids.
512 Therefore, this difference can most likely be attributed to the experimental error in the column
513 investigations and their modeling rather than to an actual effect caused by the colloids. The
514 situation, however, is very different at pH = 8 for the faster flow rate, where a steeper tailing of the
515 breakthrough curve can be seen in the absence of colloids (Figure 7), implying that a higher
516 retention of neptunium(V) in the column occurs in the presence of colloids. This is also supported
517 by the modeled K_d values which are larger in the presence of colloids than in the absence of them
518 by a factor of almost 40. As there is almost no retention to be seen on the granite in the absence of
519 colloids, the enhanced uptake by the colloids could be related to the adsorption of colloids on the

column material, providing further sorption sites for neptunium(V) attachment inside the column. Alternatively, colloids may interrupt the flow path, reducing the accessible flow channels for neptunium(V) and therefore influence the breakthrough properties of neptunium(V). Such a clogging phenomenon of colloids was observed by Missana et al (2008). When looking at the colloid breakthrough curve at this flow velocity and pH, a similar oscillating behavior can be seen as for the lower flow velocity of 0.3 mL/h. However, the recovery never reaches 100 % (oscillation occurs between 70 and 90 %) and there is no decrease of the colloid recovery as observed for the slower flow velocity. Thus, a clogging phenomenon cannot be confirmed based on the colloid breakthrough data and we must explore the possibility of colloid attachment on the column material resulting in the retention of colloid-borne neptunium(V) in the column. The point of zero charge or isoelectric point of granite has been reported to lie around pH 8 – 9 (Charalambos P., 2001; Chen T. et al., 2013). The IEP for bentonite colloids is much lower. In fact, we measured a constant negative charge of montmorillonite over the entire examined pH-range of 3-11 (Elo et al., 2017). At pH 8 some of the surface groups on granite still carry a positive charge, thus, enabling the electrostatic attachment of colloids on the surface. At pH 10 such electrostatic attachment will be decreased due to the larger amount of negatively charged surface groups. However, if pH-dependent colloid attachment on granite occurs, the effect should be visible also at pH 8, which is not the case in our column experiments. Thus, a definite conclusion of the underlying reasons for the decreased breakthrough of neptunium(V) in the presence of colloids at pH 8 and the flow velocity of 0.8 mL/h cannot be given.

4 CONCLUSIONS

In this study, we investigated the influence of MX-80 bentonite colloids on neptunium(V) migration in granite media. Neptunium(V) uptake by crushed granite was found to be pH-dependent, whereas neptunium(V) uptake by MX-80 bentonite colloids was pH-independent, unlike observed for montmorillonite purified from the MX-80 bentonite. The column experiments under flowing water conditions were conducted for chloride as a non-sorbing tracer and for neptunium(V) at two pH values (pH = 8 and 10) and two flow rates (0.3 mL/h and 0.8 mL/h). The resulting breakthrough curves were thereafter modeled using the analytical solution of advection–matrix diffusion equation in cylindrical coordinates. The modeling results of chloride breakthrough curves indicated that the flow field consisted of flowing and stagnant water and that tail of the breakthrough curve was caused by matrix diffusion into the stagnant water and later back into flowing water. The modeling results for neptunium(V) breakthrough curves were in good agreement with the experimental results. A tailing of neptunium(V) breakthrough curves in comparison to the conservative tracer was observed, which could be explained by a higher retardation of neptunium(V) in the column caused by sorption on the granite. The sorption was in general lower at pH 8 than at pH 10. In addition, the tailing was almost identical in the absence and presence of MX-80 bentonite colloids, implying that the influence of colloids on the neptunium(V) mobility is almost negligible. With respect to conditions in the repository environment where pH ranges from circumneutral to slightly alkaline, and the groundwater is mildly oxic e.g. due to the glacial melt waters, the migration of neptunium(V) is favored due to low sorption onto granite media. Therefore, at low flow rates matrix diffusion becomes an important process retarding neptunium migration under oxic conditions.

Acknowledgements. This research was financially supported by the European Atomic Energy community's Seventh Framework Programme (FP7/2007–2011) under grant agreement n° 295487 and Finnish Research Programme on Nuclear Waste Management (KYT 2018).

5 REFERENCES

Alonso U., Missana T., Geckeis H., García-Gutierrez M., Turrero M. J., Möri R., Schäfer T., Patelli A. and Rigato V., 2006. Role of inorganic colloids generated in a high-level deep geological repository in the migration of radionuclides; open questions. J. Iber. Geol., Research and development for the deep geological disposal of radioactive wastes; I, 32 (1), 79–94.

Artinger R., Kienzler B., Schüßler,W. and Kim J.I., 1998. Effects of humic substances on the ^{241}Am migration in a sandy aquifer: Column experiments with Gorleben groundwater/sediment systems. J. Contam. Hydrol. 35, 261–275.

Bachmaf S., Planer-Friedrich B. and Merkel B. J., 2008. Effect of sulfate, carbonate, and phosphate on the uranium(VI) sorption behavior onto bentonite. Radiochim. Acta 96, 359–366.

Baik M. H., Cho W. J. and Hahn P. S., 2007. Erosion of bentonite particles at the interface of a compacted bentonite and a fractured granite. Eng. Geol. 91**,** 229–239.

Bastug T., and Kuyucak S., 2005. Temperature dependence of the transport coefficients of ions from molecular dynamics simulations. Chem. Phys. Lett. 408, 84–88.

Begg J. D., Zavarin M., Tumey S. J. and Kersting A. B., 2015. Plutonium sorption and desorption behavior on bentonite, J. Environ. Radioact. 141, 106–114.

Buckau G., Artinger R., Fritz P., Geyer S. Kim J. I. and Wolf M., 2000. Origin and mobility of humic colloids in the Gorleben aquifer system. Appl. Geochem. 15, 171–179.

Buddemeier R.W. and Hunt J.R., 1988. Transport of colloidal contaminants in groundwater: radionuclide migration at the Nevada Test Site. Appl. Geochem. 3, 535–548.

Charalambos P., 2001. Cation and anion sorption on granite from the Project Shoal Test Area, near Fallon, Nevada, USA. Advances in Environmental Research, 5, 151 – 166.

Chen T., Li C., Liu X.Y. and Wang L.H., 2013. Migration study of iodine in Beishan granite by a column method. J Radioanal Nucl Chem, 298, 219 – 225.

Degueldre C., Baeyens B. and Goerlich W. 1988. Colloids in water from a subsurface fracture in granitic rock, Grimsel Test Site, Switzerland. Geochim. Cosmochim. Acta. 53, 603 – 610.

Degueldre C., Grauer R. and Laube A., 1996. Colloid properties in granitic groundwater systems. II: stability and transport study. Appl. Geochem. 11, 697–710.

Dittrich T. M., Boukhalfa H., Ware S. D. and Reimus P. W., 2015. Laboratory investigation of the role of desorption kinetics on americium transport associated with bentonite colloids. J. Environ. Radioact. 148, 170–182.

Elo O., 2014. Neptunium sorption on corundum, montmorillonite and bentonite colloids. Master's Thesis, University of Helsinki.

599 Elo O., Muller K., Bok F., Ikeda-Ohno A., Scheinost A. C., Hölttä P. and Huittinen N., 2017. Batch
600 sorption and spectroscopic speciation studies of neptunium uptake by montmorillonite and
601 corundum. Geochim. Cosmochim. Acta 198, 168–181.

602 Finn P. A., Bates J. K., Hoh J. C., Emery J. W., Hafenrichter L. D., Buck E. C. and Gong M. 1994.
603 Elements Present in Leach Solutions from Unsaturated Spent Fuel Tests. In: Scientific basis for
604 nuclear waste management XVII, MRS Proceedings 333, 399–404.

605 García-García S., Wold S. and Jonsson M., 2007. Kinetic determination of critical coagulation
606 concentration for sodium and calcium montmorillonite colloids in NaCl and $CaCl_2$ aqueous
607 solutions. J. Colloid Interface Sci. 315, 512–519.

608 Geckeis H., Schäfer T., Hauser W., Rabung Th. Missana T., Degueldre C., Möri A., Eikenberg J.,
609 Fierz Th. and Alexander W. R., 2004. Results of the colloid and radionuclide retention
610 experiment (CRR) at the Grimsel Test Site (GTS), Switzerland – impact of reaction kinetics
611 and speciation on radionuclide migration. Radiochim. Acta 92, 765–774.

612 Huber F., Kunze P., Geckeis H. and Schäfer T., 2011. Sorption reversibility kinetics in the ternary
613 system radionuclide–bentonite colloids/nanoparticles–granite fracture filling material. Appl.
614 Geochem. 26, 2226–2237.

615 Hummel W. 2008. Radioactive contaminants in the subsurface: the influence of complexing ligands
616 on trace metal speciation. Monatsh. Chem. 139, 459–480.

617 Hursthouse A. S., Baxter M. S., Livens F. R. and Duncan H. J., 1991. Transfer of Sellafield-
618 Derived Np-237 to and within the Terrestrial Environment. J. Environ. Radioact. 14, 147–174.

619 Hölttä P., Hakanen M., Hautojärvi A., Timonen J. and Väätäinen K., 1996. The Effects of Matrix
620 Diffusion on Radionuclide Migration in Rock Column Experiments. J. Contam. Hydrol.
621 21165–173.

622 Hölttä P., Siitari-Kauppi M., Hakanen M., Huitti T., Hautojärvi A., and Lindberg A., 1997.
623 Radionuclide transport and retardation in rock fracture and crushed rock colum experiments. J.
624 Contam. Hydrol. 26, 135–145.

625 Hölttä P., Poteri A., Hakanen M. and Hautojärvi A., 2004. Fracture flow and radionuclide transport
626 in block–scale laboratory experiments. Radiochim. Acta 92, 775–779.

627 Hölttä P., Siitari-Kauppi M., Leskinen A. and Poteri A., 2008. Retardation of mobile radionuclides
628 in granitic rock fractures by matrix diffusion. Phys. Chem. Earth. 33, 983–990.

629 Ikonen J., Voutilainen M., Söderlund M., Jokelainen L., Siitari-Kauppi M. and Martin A., 2016.
630 Sorption and diffusion of selenium oxyanions in granitic rock. J. Contam. Hydrol. 192, 203–
631 211.

632 Jansson M. 2009. Bentonite erosion, Laboratory studies. SKB Technical Report TR-09-33.

633 Jokelainen L., Ikonen J., Read D., Hellmuth K.-H. and Siitari-Kauppi M., 2009. The diffusion of
634 tritiated water, chloride and uranium through granite. In: Scientific basis for nuclear waste
635 management XXXIII, MRS Proceedings 1193, 461–468.

636 Kaszuba J. P. and Runde W. H., 1999. The aqueous geochemistry of neptunium: dynamic control of
637 soluble concentrations with applications to nuclear waste disposal. Environ. Sci. Technol. 33,
638 4427–4433.

639 Kekäläinen P., Voutilainen M., Poteri A., Hölttä P., Hautojärvi A. and Timonen J., 2011. Solutions
640 to and validation of matrix-diffusion models. Transp. Porous Med. 87 (1), 125–149

641 Kekäläinen P., 2014. Analytical solutions to matrix diffusion problems. AIP Conference
642 Proceedings, 1618, 513–516.

643 Kersting A.B., Efurd D. W., Finnegan D.L., Rokop D.J., Smith D.K. and Thompson J.L., 1999.
644 Migration of plutonium in ground water at the Nevada Test Site. Nature 397, 56–59.

645 Kienzler B., Vejmelka P., Romer J., Fanghänel E., Jansson M., Eriksen T.E. and Wikberg P., 2003.
646 Swedish-German actinide migration experiment at ÄSPÖ hard rock laboratory. J. Contam.
647 Hydrol. 61, 219–233

648 Kumata M. and Vandergraaf T. T., 1998. Experimental study on neptunium migration under in situ
649 geochemical conditions. J. Contam. Hydrol. 35, 31–40.

650 Kumpulainen S. and Kiviranta L., 2010. Mineralogical and chemical characterization of various
651 bentonite and smectites rich clay materials. Posiva Working Report, 2010–52.

652 Kuva J., Voutilainen M., Kekäläinen P., Siitari-Kauppi M., Sammaljärvi J., Timonen J. and
653 Koskinen L., 2016. Gas phase measurements of matrix diffusion in rock samples from
654 Olkiluoto bedrock, Finland. Transp. Porous Med. 115, 1–20.

655 Laaksoharju M. and Wold S. 2005. The colloid investigations conducted at the Äspö Hard Rock
656 Laboratory during 2000–2004. SKB Technical Report TR-05-20.

657 Lagaly G. and Ziesmer S., 2003. Colloid chemistry of clay minerals: the coagulation of
658 montmorillonite dispersions. Adv. Colloid Interface Sci. 100-102, 105–128.

659 Lahtinen M., Hölttä P., Riekkola M.L., Yohannes G. 2010, Analysis of colloids released from
660 bentonite and crushed rock. Physics & Chemistry of the Earth - Parts A/B/C, 35, 265 – 270.

661 Li P., Liu Z., Ma F., Shi Q. L., Guo Z. J. and Wu W. S., 2015. Effects of pH, ionic strength and
662 humic acid on the sorption of neptunium(V) to Na-bentonite. J. Mol. Liq. 206, 285–292.

663 Moreno L, Gylling B and Neretnieks, I., 1997. Solute transport in fractured media the important
664 mechanisms for performance assessment. J Contam Hydrol 25, 283-298.

665 Missana T., Alonso U. and Turrero M. J., 2003. Generation and stability of bentonite colloids at the
666 bentonite/granite interface of a deep geological radioactive waste repository. J. Contam.
667 Hydrol. 61, 17–31.

668 Missana T., García-Gutiérrez M. and Alonso U., 2004. Kinetics and irreversibility of cesium and
669 uranium sorption onto bentonite colloids in a deep granitic environment. Appl. Clay Sci. 26,
670 137–150.

671 Missana T., Alonso U., García-Gutiérrez M. and Mingarro M., 2008. Role of bentonite colloids on
672 europium and plutonium migration in a granite fracture, Appl. Geochem. 23, 1484–1497.

673 Missana T., Alonso U., Albarran N., García-Gutierrez M. and Cormenzana J. l., 2011. Analysis of
674 colloids erosion from the bentonite barrier of a high level radioactive waste repository and
675 implications in safety assessment. Phys. Chem. Earth. 36, 1607–1615.

676 Möri A., Alexander W. R., Geckeis H., Hauser W., Schäfer T., Eikenberg J., Fierz Th., Dequeldre
677 C. and Missana T., 2003. The colloid and radionuclide retardation experiment at the Grimsel
678 Test Site: influence of bentonite colloids on radionuclide migration in a fractured rock.
679 Colloids Surf. A: Physicochem. Eng. Aspects 217, 33–47

680 Niemiaho S., 2013. Bentoniittikolloidien kulkeutuminen ja vaikutus Sr-85 ja Eu-152 liikkuvuuteen
681 graniittisessa kivessä. Master's Thesis, University of Helsinki.

682 Novikov A. P., Kalmykov S. N., Utsunomiya S., Ewing R. C., Horreard F., Merkulov A., Clark S.
683 B., Tkachev V. V. and Myasoedov B. F., 2006. Colloid Transport of Plutonium in the Far-Field
684 of the Mayak Production Association, Russia. Science 314, 638–641.

685 Park C., Kienzler B., Vejmelka P. and Jeong J., 2012. Modeling and analysis of the migration of
686 HTO and ^{237}Np in a fractured granite core at the Äspö hard rock laboratory. Radiochim. Acta
687 100 (3) 197-205.

688 Puls R. W. and Powell R. M., 1992. Transport of Inorganic Colloids through Natural Aquifer
689 Material: Implications for Contaminant Transport. Environ. Sci. Technol. 26, 614–621.

690 Ren X., Wang S., Yang S. and Li J., 2010. Influence of contact time, pH, soil humic/fulvic acids,
691 ionic strength and temperature on sorption of U(VI) onto MX-80 bentonite, J. Radioanal. Nucl.
692 Chem. 283, 253–259.

693 Ryan J.N. and Elimelech M., 1996. Colloid mobilization and transport in groundwater. Colloids
694 Surf. A 107, 1–56.

695 Sabodina M. N., Kalmykov S. N., Sapozhnikov Y. A. and Zakharova E. V., 2006. Neptunium,
696 plutonium and 137Cs sorption by bentonite clays and their speciation in pore waters, J.
697 Radioanal. Nucl. Chem. 270, 349–355.

698 Schäfer T., Geckeis H., Bouby M. and Fanghänel T., 2004. U, Th, Eu and colloid mobility in a
699 granite fracture under near-natural flow conditions. Radiochim. Acta 92, 731–737.

700 Schäfer T., Huber F., Seher H., Missana T., Alonso U., Kumke M., Eidner S., Claret F. and
701 Enzmann F. 2012. Nanoparticles and their influence on radionuclide mobility in deep
702 geological formations. Appl. Geochem. 27, 390 – 403.

703 Short S.A., Lowson R.T. and Ellis J., 1988. U^{234}/U^{238} and Th^{230}/U^{234} activity ratios in the colloidal
704 phases of aquifers in lateritic weathered zones. Geochim. Cosmochim. Acta 52, 2555–2563.

705 Smith P.A. and Degueldre. 1993. Colloid-facilitated transport of radionuclides through fractured
706 media. J. Contam. Hydrol. 13, 143 – 166.

Tombácz E. and Szekeres M., 2004. Colloidal behavior of aqueous montmorillonite suspensions: the specific role of pH in the presence of indifferent electrolytes. Appl. Clay Sci. 27, 75–94.

Torok J., Buckley L.P., Woods B.L., 1990. The separation of radionuclide migration by solution and particle transport in soil. J. Contam. Hydrol. 6, 185–203.

Verma P. K., Pathak P. N., Mohapatra P. K., Godbole S. V., Kadam R. M., Veligzhanin A. A., Zubavichus Y. V. and Kalmykov S. N., 2014. Influences of different environmental parameters on the sorption of trivalent metal ions on bentonite: batch sorption, fluorescence, EXAFS and EPR studies. Environ. Sci.: Processes Impacts 16, 904–915.

Verma P. K., Romanchuk A. Y., Vlasova I. E., Krupskaya V. V., Zakusin S. V., Sobolev A. V., Egorov A. V., Mohapatra P. K. and Kalmykov S. N., 2017. Neptunium(V) uptake by bentonite clay: Effect of accessory Fe oxides/hydroxides on sorption and speciation, Appl. Geochem. 78, 74–82.

Vilks P., Cramer J.J., Bachinski D.B., Doern D.C. and Miller, H.G., 1993. Studies of colloids and suspended particles, cigar lake uranium deposit, Saskatchewan, Canada. Appl. Geochem. 8, 605–616.

Vilks P. and Baik M., 2001. Laboratory migration experiments with radionuclides and natural colloids in a granite fracture. J. Contam. Hydrol. 47, 197–210.

Voutilainen M., Kekäläinen P., Poteri, A., Siitari-Kauppi M., Yli-Kaila M. and Koskinen L., 2018. Advection-matrix diffusion experiments in in situ and laboratory conditions. Submitted to publication.

Zhao D. L., Feng S. J., Chen C. L., Chen S. H., Xu D. and Wang X. K., 2008. Adsorption of thorium(IV) on MX-80 bentonite: Effect of pH, ionic strength and temperature, Appl. Clay Sci. 41, 17–23.

Zhao P., Tinnacher R. M., Zavarin M. and Kersting A. B., 2014. Analysis of trace neptunium in the vicinity of underground nuclear tests at the Nevada National Security Site. J. Environ. Radioact. 137, 163–172.

Zong P., Wu X., Gou J., Lei X., Liu D. and Deng H., 2015. Immobilization and recovery of uranium(VI) using Na-bentonite from aqueous medium: equilibrium, kinetics and thermodynamics studies. J. Mol. Liq. 209, 358–366.